



# 1 Transformations in Exposure to Debris Flows in Post-Earthquake Sichuan, 2 China

3  
4 Isabelle Utley<sup>1</sup>, Tristram Hales<sup>1</sup>, Ekbal Hussain<sup>2</sup>, Xuanmei Fan<sup>3</sup>

5  
6 [1] School of Earth and Environmental Sciences, Cardiff University, Cardiff, CF10 3AT, UK.

7 [2] British Geological Survey, Keyworth, Nottingham, NG12 5GG, UK

8 [3] State Key Laboratory of Geohazard Prevention, Chengdu University of Technology, Chengdu, China

9  
10 Correspondence to: Isabelle E.K Utley ([ieku20@bath.ac.uk](mailto:ieku20@bath.ac.uk))

11  
12 **Abstract.** Post-earthquake debris flows can exceed volumes of  $1 \times 10^6 \text{m}^3$  and pose significant challenges to  
13 downslope recovery zones. These stochastic hazards form when intense rain remobilises coseismic landslide  
14 material. We investigate the relationship between changing exposure and hazard of post-2008 debris flows in  
15 three gullies in Sichuan province, China. These were selected based on the number of post-earthquake check dams  
16 – Cutou (2), Chediguan (2) and Xiaojia (none). Using high resolution satellite images, we developed a  
17 multitemporal building inventory from 2005 to 2019, comparing it to spatial distribution of previous debris flows  
18 and future modelled events. Post-earthquake urban development in Cutou and Chediguan increased exposure to a  
19 major debris flow in 2019 with inundation impacting 40% and 7% of surveyed structures respectively. We  
20 simulated future debris flow runouts using LAHARZ to investigate the role of check dams in mitigating three  
21 flow volumes –  $10^4 \text{m}^3$  (low),  $10^5 \text{m}^3$  (high) and  $10^6 \text{m}^3$  (extreme). Our simulations show check dams effectively  
22 mitigate exposure to low and high flow events but prove ineffective for extreme events with 59% of buildings in  
23 Cutou, 22% in Chediguan and 33% in Xiaojia significantly affected. We verified our analyses through employing  
24 a statistical exposure model, adapted from a social vulnerability equation. Cutou's exposure increased by 64% in  
25 2019, Chediguan's by 52% whilst only 2% for Xiaojia in 2011, highlighting that extensive grey infrastructure  
26 correlates with higher exposure to extreme debris flows, but less so to smaller events. Our work suggests the  
27 presence of check dams increases the perception of exposure reduction downstream, however, ultimately produces  
28 a levee effect that raises exposure to large events.

## 29 30 **Keywords**

31 Debris Flows, Built Environment, Exposure, Check dams, LAHARZ.

## 32 33 34 **1. Introduction**

35 Major earthquakes such as the 1994  $M_w$  6.8 event in Northridge, California (Harp and Jibson, 1996) and the 1999  
36  $M_w$  7.3 earthquake in Chi-Chi, Taiwan (Liu et al., 2008) have triggered chains of hazards, that increase the  
37 exposure of local communities to secondary hazards for many years after the initial disaster. Following the 2008  
38  $M_w$  7.9 Wenchuan earthquake in Sichuan, China, debris flows occurred more frequently and at a higher magnitude  
39 ( $>1 \times 10^6 \text{m}^3$ ) after the earthquake compared to flows before the earthquake (Cruden and Varnes., 1996; Cui et al.,  
40 2008; Huang and Li., 2009; Guo et al., 2016; Thouret et al., 2020). Increased debris flow frequency impacts  
41 vulnerable communities and local infrastructure, potentially reshaping the demographic and structural landscape  
42 of previously rural regions (Chen et al., 2011). The frequency of post-seismic flows is heavily influenced by  
43 sediment availability which is often controlled by coseismic landslide distribution, hydrology, and slope (Horton  
44 et al., 2019). The ready transformation and remobilisation of seismically loosened deposits into water-laden  
45 sediments leads to a heightened probability of debris flow hazard for extended periods, further exacerbating the  
46 potential impacts felt by these areas (Costa et al., 1984; Huang & Li, 2014; Fan et al., 2019b).

47  
48 Post-seismic debris flows affect the expanding built environment and communities located in the flat land that  
49 forms along floodplains and on debris and alluvial fans. In addition to direct loss of life, debris flows repeatedly  
50 block and/or destroy rivers, roads, tunnels, and bridges, and damage property and agriculture, and loss of life  
51 (Chen, N et al., 2011). Buildings are highly susceptible to the impacts of debris flows (Hu et al., 2012; Zeng et  
52 al., 2015), with property damage responsible for nearly all impacts i.e., casualties and fatalities (Wei et al., 2018;  
53 Wei et al., 2022). Variations in construction material are a particularly important factor for structural resilience  
54 and vulnerability to debris flows (Zhang, S et al., 2018). Despite focus on building resilience and reducing  
55 vulnerability, post-earthquake regions are often areas of significant rebuilding and expansion of infrastructure so  
56 the exposure to debris flows changes rapidly in these areas. The development of critical infrastructure such as  
57 highways and tunnels further encourage the growth of the built environment and subsequent influx of people  
58 settling in areas exposed to geological hazards (Cruden and Varnes, 1996; Jiang et al., 2016).



59  
60 Check dams are a common form of risk mitigation for debris flows globally (Zeng et al., 2009; Peng et al., 2014;  
61 Cucciaro, S. et al., 2019b), and one that is prevalent in post-earthquake Wenchuan (Chen, X. et al., 2015; Guo  
62 et al., 2016). Check dams store debris flow sediment, locally reduce channel slope, and are often permeable to  
63 affect debris flow hydrology. However, they have significant disadvantages such as requiring regular maintenance  
64 (to reduce sediment inputs) (Kean et al., 2018). The mitigation potential of these structures is contingent on their  
65 position along a channel, their height, amount of sediment fill, and their strength (which depends on the materials  
66 used for construction) (Dai et al., 2017). These factors evolve through time, meaning that the hazard mitigating  
67 factor of check dams varies through time and with unknown sign. The presence of check dams changes the  
68 downstream risk, primarily through changing the magnitude and frequency distribution of debris flows within the  
69 channel. For well-made check dams of sufficient volume to mitigate the largest debris flows, this can reduce the  
70 downstream risk of debris flows to negligible by effectively mitigating the entire hazard. However, in the case of  
71 the Wenchuan region, check dams are rarely large enough or regularly cleared of sediment to mitigate the largest  
72 debris flows, which can exceed  $10^6$  m<sup>3</sup>-in volume.  
73

74 The presence of check dams, particularly in drainage basins with a limited history of catastrophic debris flow  
75 events may affect the perception of risk downstream. They serve to stabilize, obstruct, drain, and/or halt the  
76 movement of flows (Hübl and Fiebiger., 2005; Chen et al., 2015). The perception that check dams have mitigated  
77 all hazards may promote the expansion of infrastructure into floodplains and debris fans. The increase of exposure  
78 is common on floodplains where the presence of flood control levees can promote building onto floodplains – a  
79 process that is called the levee effect (Collette et al., 2015). In the flooding example, the presence of levees  
80 reduces the frequency of small and medium sized floods, but when large floods occur that cause those levees to  
81 fail, heightened floodplain exposure can lead to higher damage. The effect of check dams on risk perception is  
82 less well understood. Anecdotal examples from the Wenchuan region (e.g., Hongchun, Taoguan gullies) show  
83 that large debris flow events in 2010, 2013 and 2019 caused significant damage despite the presence of check  
84 dams (Dai et al., 2017). However, it is not clear if the presence of check dams affected exposure relative to the  
85 large-scale expansion of infrastructure in the post-earthquake recovery phase.  
86

87 This study seeks to understand the changing exposure to debris flows in post-earthquake Wenchuan communities.  
88 We compare the exposure of buildings to debris flow events in two neighbouring catchments containing check  
89 dams (Cutou and Chediguan) using a third, unmitigated gully as a control measure (Xiaoja). We compare post-  
90 2008 built environment growth across the 3 catchments and compare the potential exposure of infrastructure in  
91 each gully to debris flow events of different sizes.  
92

## 93 94 **2. Study Area: Sichuan Province, China**

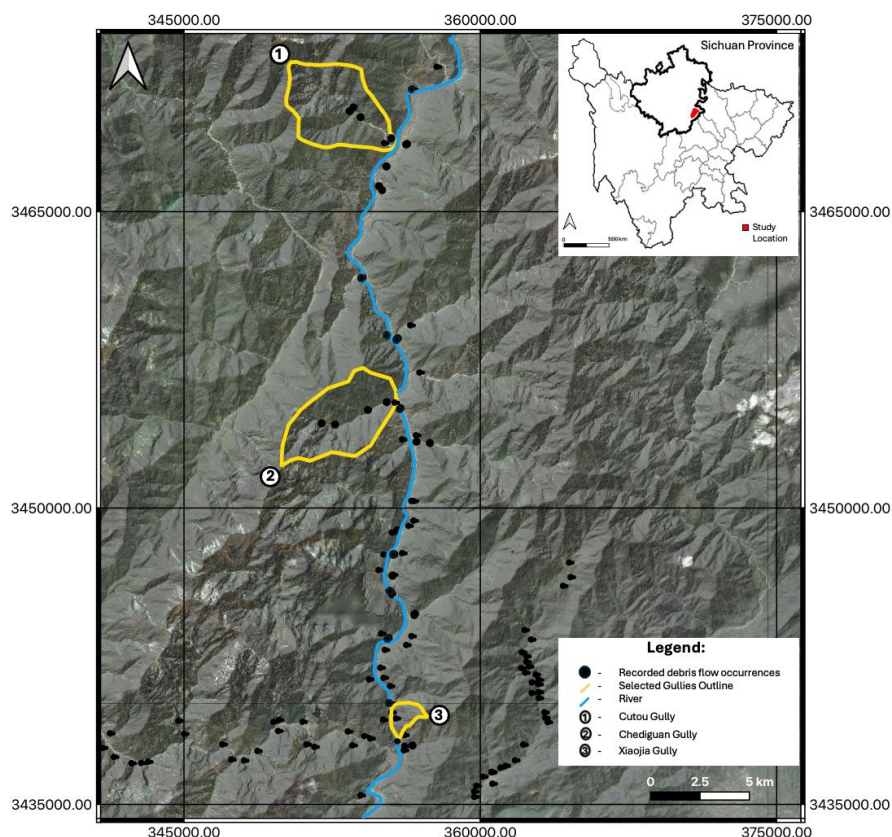
95 China's mountainous regions, including the Longmenshan, account for 69% of the country's land mass with over  
96 a third of the population living in these regions (Chen et al., 2011; He et al., 2022). 72% of this landscape suffers  
97 from debris flow activity. Between 2005 and 2018, estimates suggest over 800 debris flow occurrences each year  
98 (He et al., 2022; Wei et al., 2021). Of these, landslides dominate provinces in the North and debris flows are  
99 generally constrained to provinces in the South (Liu et al., 2018). The 2008 Mw 7.9 Wenchuan earthquake  
100 primarily impacted Sichuan province (Fig 1). The epicentre was located near Yinxiu, Wenchuan County, within  
101 the seismically active Longmenshan Fault Zone (Li et al., 2019). The shaking triggered around 56,000 landslides  
102 and displaced nearly 3 km<sup>3</sup> of loose material (Fan et al., 2018; Luo et al, 2020). In subsequent years, the unstable  
103 material has been reactivated as debris flows, many of which exceed  $10^6$  m<sup>3</sup> in mobilised volume (Frances et al.,  
104 2022). The risk from these debris flows has been compounded by increasing exposure due to China's rapid rural  
105 development programme, which includes the construction of roads, bridges, and industrial facilities (Tang et al.,  
106 2022).  
107

108 Four significant episodes of debris flows occurred in the post-earthquake Wenchuan region in 2008, 2010, 2013  
109 and 2019 (Tang et al., 2022; Fan et al., 2019b). Each event was associated with monsoon rainfall that occurred in  
110 different parts of the range. The largest flow surges, containing millions of cubic meters of sediment were located  
111 in the gullies along the Minjiang in Sichuan. Large scale flooding further amplified the impacts, for example in  
112 Yingxiu Town, Wenchuan County (Liu et al., 2016b). Debris flow events occurring post-earthquake often exhibit  
113 larger material volumes compared to flow events recorded prior to 2008. Horton et al., (2019) attributed the  
114 increase in flow volume to the large-scale displacement of sediment during the earthquake. The resulting increase  
115 in debris flow hazards necessitated, engineered mitigation measures to reduce risk levels in the basin communities  
116 (Tang et al., 2009; Huang et al., 2009; Huang, 2012).  
117



118 In this study we focus on three gullies along the Minjiang - Cutou, Chediguan and Xiaojia and debris flow events  
119 on August 20<sup>th</sup>, 2019, and 4<sup>th</sup> July 2011 (Fig 1). Cumulative rainfall on 20<sup>th</sup> August 2019 peaked at 83 mm in  
120 Cutou and 65 mm in Chediguan resulting in large debris flows measuring over  $50 \times 10^4 \text{ m}^3$  in each gully. Cutou  
121 gully is known for its high frequency of post-seismic debris flows, which has been attributed to the total of  $11 \times 10^6$   
122  $\text{m}^3$  coseismic deposits generated by the earthquake (Yan et al 2014). Although a check dam was built in 2011 to  
123 manage debris flow impacts in Chediguan gully a large damaging debris flow of  $64 \times 10^4 \text{ m}^3$  occurred on 20 August  
124 2019 and destroyed the drainage groove and G213 Taiping Middle Bridge (Li et al., 2021). The debris briefly  
125 blocked river flow in the Minjiang causing water levels to rise during flood peak. This led to flooding at the  
126 Taipingyi hydropower station located 200 m upstream.  
127

128 Xiaojia gully, is a moderate debris flow hazard area based on limited past occurrences and has no existing  
129 engineered mitigation measures. Following a period of debris flow activity in 2010, and after a period of  
130 continuous heavy rainfall approximately  $30,000 \text{ m}^3$  of deposits were remobilised and transported along the channel  
131 to the gully mouth. This event led to a period of disruption on the S303 road from flooding (Liu et al., 2014).  
132

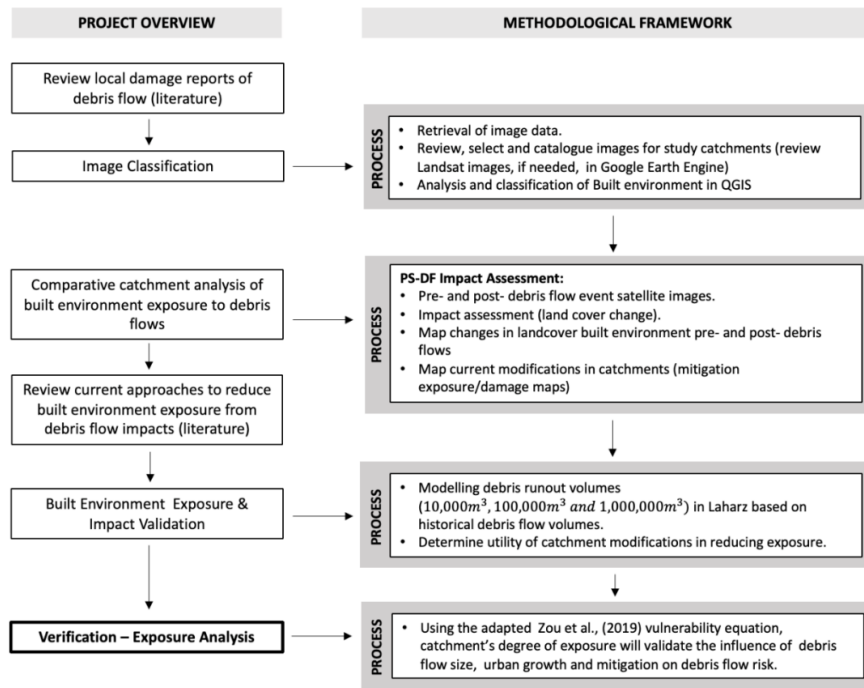


133  
134 **Figure 1:** Location of the three gullies that form the focus of this study within Sichuan Province. Recorded post-  
135 2008 landslide occurrences are from the Wang et al. (2022) multitemporal datasets (© Google Earth 2019).  
136  
137

138  
139  
140  
141  
142



143 **3. Methodology**  
 144



145 **Figure 2:** Schematic of our method. The key data sources comprise three multi-temporal datasets, including two  
 146 from Fan et al. (2019a) covering debris flow and triggering rainfalls, as well as mitigation measures. The third  
 147 dataset is adapted from Fan et al., (2019a) and highlights gully's with debris flow events post-2008 including  
 148 information on the flow volume and presence of mitigation. Additional spatial data sources include aerial imagery  
 149 from OpenStreetMap (OpenStreetMap contributors., 2023), World Settlement Footprint (World Settlement  
 150 Footprint., 2019) and Shuttle Radar Topography Mission (SRTM) (Farr et al, 2007).  
 151  
 152

153  
 154 **3.1 Data Classification**  
 155

156 This study builds on existing multi-temporal debris flow datasets produced by Fan et al., (2019a). Dataset 1 has  
 157 an aerial extent of 892 km<sup>2</sup> and presents the location and dimensions of debris flow events between 2008 and  
 158 2020. Dataset 2 presents a list of mitigative actions e.g., construction of check dams, taken between 2008–2011.  
 159 We used an SRTM DEM to construct elevation profiles of Cutou, Chediguan and Xiaojia gullies to extract  
 160 topographic characteristics to understand the mechanism of slope failure in the event of a rainfall-induced debris  
 161 flow. These profiles facilitate morphological valley changes from debris flows to be identified. Through a  
 162 comparative analysis of the 20<sup>th</sup> August 2019 debris flows in Cutou and Chediguan, we investigated the relative  
 163 difference in land use change in the two gullies from 2008 to 2019, with a focus on changes before and after the  
 164 2019 flow event.

165 Landscape modification from 2005 to 2019 were mapped using high resolution (0.5 to 2.5m) satellite images  
 166 (Table 1). We selected images with less than 50% cloud cover and cross-referenced the mapped features with  
 167 existing data sources in OpenStreetMap (OpenStreetMap contributors., 2023) and Dynamic World (Brown et al.,  
 168 2022). Where satellite imagery was unavailable, we used aerial photos obtained from Google Earth,  
 169 OpenStreetMap and World Settlement Footprint (World Settlement Footprint., 2019). It should be acknowledged  
 170 that platforms like OpenStreetMap offer a regional view of Wenchuan rather than a detailed local-scale with  
 171 mapping limited to main roads and 150 settlement polygons. However, this study's locations are unaffected by  
 172 this due to their position next to the G213 national highway and G4217 road.  
 173



174  
175

**Table 1** Satellite and aerial imagery used for data analysis and interpretation of the built environment

Data ID	Data Source	Acquisition Date	Resolution (m)
Aerial Satellite	Worldview (in QGIS – ‘Satellite’ XYZ tile)	2022	1.0
Satellite	Worldview (in Google Earth Pro., 2023)	10.12.2010 26.04.2011 03.04.2018 29.10.2019	1.0
Satellite	Planet	14.08.2019 24.08.2019	3.0
Satellite	Maxar Technologies (in Google Earth Pro., 2023)	09.09.2005 26.04.2011	3.0
Satellite	CNES/Airbus (in Google Earth Pro., 2023)	15.04.2015	1.0

176  
177  
178  
179  
180  
181  
182  
183  
184

We mapped features corresponding to human activities such as roads and properties. We highlighted at-risk zones in Cutou, Chediguan, and Xiaojia. We focus on spotlighting areas of high debris flow exposure in Cutou and Chediguan, comparing them with Xiaojia to evaluate the efficacy of check dams in mitigating potential debris flow hazards downstream of the dams.

### 3.2 Modelling Future Debris Flow Runout and Building Exposure

185  
186  
187  
188  
189  
190  
191  
192  
193  
194  
195  
196  
197  
198  
199

Both Cutou and Chediguan had check dams installed after the 2008 earthquake. We compared the impacts of 2019 debris flows in Cutou and Chediguan gullies with a 2011 debris flow event in the unmodified Xiaojia gully to identify the effectiveness of artificial dams in mitigating exposure to post-seismic debris flows. By using scenario modelling we identified at which point, does the size of the hazard, outweigh the mitigative capacity of the check dam to prevent overtopping. We mapped debris flows of differing scales within each of our three catchments using LAHARZ a GIS toolkit for lahar hazard mapping and modelling, developed by the USGS to visualise debris flow paths based on an empirical set of equations (Schilling., 2014; Iverson et al., 1998). The model provides an estimate of flow extent from a given initial material volume, and can account for various factors such as topography, slope and mitigative structures which generates more detailed data outputs when simulating future flow behaviour. For each catchment we simulated three flow sizes that represent the range of observed post-2008 earthquake debris flow volumes:  $10^4 m^3$ ,  $10^5 m^3$  and  $10^6 m^3$ . These volumes represent low, high, and extreme debris flows respectively based off of recorded post-seismic debris flow occurrences post-2008 documented in the Fan et al., (2019a) datasets. We note that there is not a strong understanding currently of what controls the maximum size of debris flows within Wenchuan catchments, hence we cannot attribute a particular probability to each scenario.

200  
201  
202  
203  
204  
205  
206

In the analysis of post-seismic debris flow, vulnerability assessment plays a crucial role (Lo et al., 2012). However, adapting traditional vulnerability methods which analyse inherent fragility and the potential loss of elements at risk, both attainable through remote practises, calculating exposure with minimal onsite data, remains a challenge. We adapted a vulnerability model by Zou et al. (2019) to quantify the extent of exposure to the built environment at our three sites, Cutou, Chediguan and Xiaojia.

207  
208  
209  
210  
211

Utilising satellite and/or aerial imagery and extracting spatial characteristics to identify both elements at risk as well as hazard-affected zones, our analysis facilitates the assessment of regional exposure without relying heavily on data collected onsite. Our model quantifies the susceptibility of the built environment to debris flow damage. The degree of exposure,  $E_{df}$ , is expressed as:

212  
213

$$E_{df} = E_b \times C \pm M \quad (1)$$

214  
215  
216  
217  
218  
219  
220  
221

$E_b$  is the number of buildings damaged, and C is the fragility index of the elements at risk (Zou et al., 2019). Fragility values range from 0 to +1, with higher values indicating greater susceptibility to damage and/or failure. We assigned fragility values through using a mixture of literature and satellite images; buildings shown to be inundated or damaged in previous events or situated along the channel or gully mouth were given a value of 1, all other buildings were set a value of 0. The key difference between our method and that of Zou et al (2019) is the incorporation a modification factor, M, to account for the effectiveness of engineered measures like check dams in mitigating building damage and subsequent exposure. The addition of this factor brings an evaluative element



222 to the exposure assessment, assigning values ranging from -1.0 to +2.0. For instance, gullies will be assigned a  
223 value of '+1' if modifications prove unsuccessful, '0' if no modifications are present, or '-1' if protection is offered  
224 by the mitigation measures. This approach, based upon the methodology proposed by Zou et al. (2019), allows  
225 for an assessment of exposure by considering both the physical resistance of buildings and the efficacy of  
226 mitigation efforts.

227  
228  
229

#### 4. Results

230  
231

##### 4.1 Assumptions

232  
233  
234  
235  
236  
237  
238  
239  
240  
241  
242

In constructing the building inventory for Cutou and Chediguan, a comprehensive approach was taken to ensure accuracy and completeness. We used aerial and satellite imagery spanning 14 years, with a focus on mapping changes from 2011 to 2019. This involved careful analysis to delineate individual buildings, considering variations in size, shape, and spatial arrangement. Mapping efforts for Xiaojia were limited to 2010-2011 due to suboptimal image quality. Our approach incorporated assumptions regarding structural categorisation, including residential, industrial, and commercial buildings. These assumptions were informed by existing literature on local building typologies and architectural styles (Hao et al., 2013; Hao et al., 2012) and aerial photograph analysis from platforms such as Google Earth and Dynamic World. By amalgamating diverse information sources, we aimed to create a comprehensive inventory that correctly reflects the built environment of the study area.

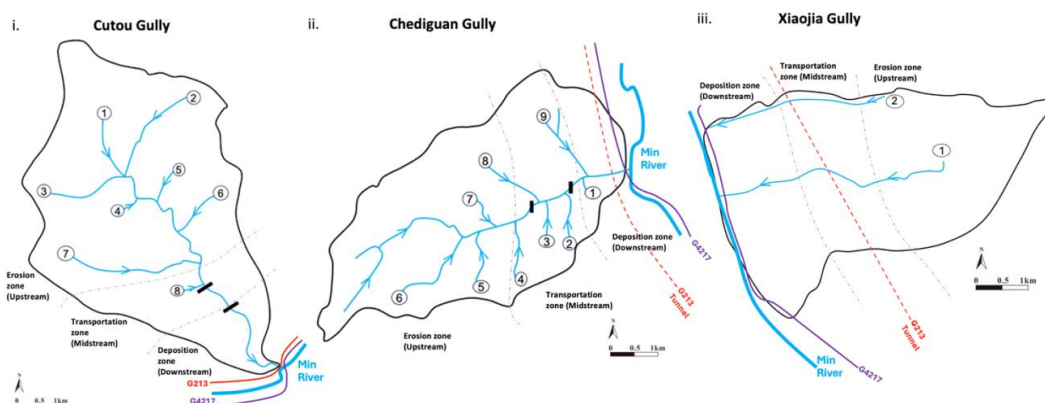
243  
244  
245  
246  
247  
248  
249  
250  
251

Additionally, we used a 30-meter Digital Elevation Model (DEM) obtained from the SRTM dataset (Farr et al., 2007). However, it is necessary to acknowledge the limitations of this data, particularly its poor resolution and subsequent blockiness, which potentially hindered detailed topographical analysis. Despite this, the DEM provided valuable contextual information for understanding the terrain and its influence on building distribution and spatial patterns within the three sites. Furthermore, while using the empirical LAHARZ model for debris flow inundation mapping, we had to account for a degree of approximation in both aerial coverage and debris flow inundation due to the 30m resolution of the DEM file.

##### 4.2 Mapping Post-Earthquake Risk

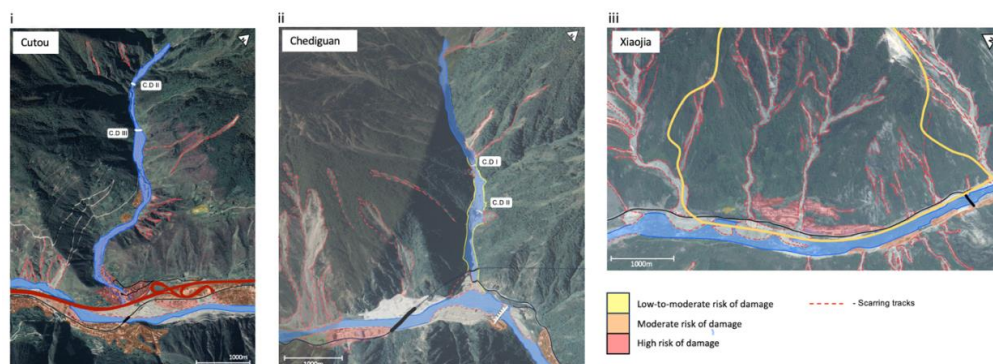
252  
253  
254  
255  
256  
257  
258  
259  
260  
261

Analysis of satellite imagery from 2005 to 2019, and topographic profiles, reveals channel widening, deepening, aggradation, and deposition, likely attributed to the mobilisation of coseismic deposits and subsequent debris flow occurrences (Zhang et al., 2015; Wang et al., 2018) (Fig 3). These observations allowed us to determine the zones of erosion, transportation, and deposition for each gully and to track changes over time. Hydrological and geomorphological analysis examines landscape morphology to identify erosional and depositional features i.e., scarring, changes to river channel, sediment buildup (Fig 4). By integrating the above, we delineated erosion-prone areas, which permitted sediment transport routes to be approximated, and identify locations of sediment deposition along the hydrological profile.



262  
263  
264  
265

**Figure 3:** Hydrological profiles for the 3 study sites. Dam locations approximated for Cutou (i) and Chediguan (ii) based on a combination satellite imagery. Streams and main tributaries are numbered. Catchment profiles have been segmented into 3 zones – ‘erosion’, ‘transportation’ and ‘deposition’ and key infrastructure annotated



266 **Figure 4:** Satellite images of the 3 study locations highlighting areas of scarring from previous debris flow activity  
267 and areas of increased erosion (© Google Earth 2019). Dam locations have been approximated for Cutou (i) and  
268 Chediguan (ii). The built environment has been shaded based upon risk of damage based upon proximity to areas  
269 of high erosion. Critical infrastructure has been added where appropriate: black like represents the G4217 road  
270 with the thicker sections representing bridges and the dashed lines, tunnels. The red line in (i) is the G213 Highway  
271

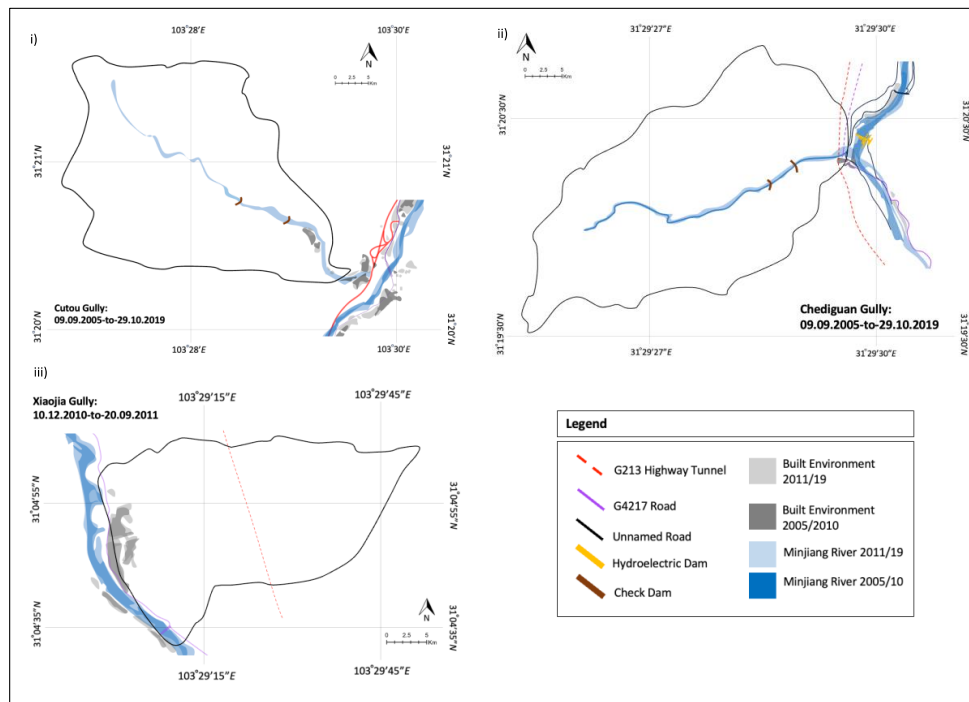
272  
273 In Cutou and Chediguan, deposition patterns shifted post-earthquake, particularly following the construction of  
274 check dams. Increased deposition occurs behind check dams compared to meander bends and basal slopes of the  
275 debris fan, demonstrating the effective sediment trapping of the check dams (Wang et al., 2019). Regarding the  
276 erosion patterns in Xiaojia, we observed common patterns in the upper gully sections at higher elevations, with  
277 deposition occurring at the basal slopes. This is due to the absence of structural alterations to the channel,  
278 permitting sediment to be transported to the channel and subsequent river outlet directly. The deposition patterns  
279 in Cutou and Chediguan, are strongly controlled by the distribution of check dams, in the middle and downstream  
280 portions of the catchment (Wang et al., 2019). The complex interplay between natural and anthropogenic factors  
281 demonstrates the dynamic evolution of risk in post-earthquake catchments and highlights the role of check dams  
282 in both mitigating and potentially exacerbating risk.  
283

284 The landscape morphology prior to the 2008 earthquake was marked by extensive vegetation (over 70% of land  
285 cover) and minimal permanent engineered features. Cutou gully contained a widespread distribution of buildings  
286 along both the mid and lower slopes. Figure 5 shows the growth of the built environment between 2005 and 2019  
287 in Cutou and Chediguan and between 2010 to 2011 in Xiaojia. The built environment in Cutou is concentrated  
288 within the transportation and deposition zones on both sides on the stream. In Chediguan by comparison we  
289 observed fewer residential structures, mostly industry and some commercial structures. Additionally, buildings in  
290 the gully are more spread out than in Cutou highlighted by the isolated settlements to the south of the catchment  
291 and single industrial site situated in the basin. Post-2008, noticeable tracks of scarring from debris flows are  
292 concentrated downstream of dams 2 and 3 in Cutou (Fig 4(i)), and upstream of dams 1 and 2 in Chediguan (Fig  
293 4(ii)). Deposition patterns are evident downstream of all modifications, forming a depositional zone,  
294 encompassing approximately 15% and 20% of the built environment in 2019 within the transportation zone of  
295 Cutou and Chediguan, respectively. In contrast, Xiaojia, lacking engineered dam structures, shows a characteristic  
296 pattern of erosion upstream and deposition downstream. Notably, between check dam structures in Cutou and  
297 Chediguan, deposition predominates on the northern channel flank, while erosion is more pronounced on the  
298 southern flank.  
299

300 Our analysis of Xiaojia unveils no discernible relationship between building development and heightened  
301 exposure, particularly to residential and critical infrastructure. This lack of correlation is potentially linked to  
302 factors beyond simple urbanisation patterns, like construction quality, building regulations, presence of natural  
303 barriers, and effectiveness of mitigation measures. To fully understand this observation, further investigation into  
304 the above variables is warranted. Additionally, detailed mapping of past debris flow events and their impacts on  
305 the built environment could provide insights into the specific mechanisms influencing vulnerability in Xiaojia.  
306 By conducting a more comprehensive analysis that considers these factors, we can gain a better understanding of  
307 the complex interactions between building development and exposure to natural hazards in Xiaojia. This, in turn,  
308 can inform more effective risk management and mitigation strategies tailored to the unique characteristics of the  
309 area. Development in Xiaojia primarily concentrates on the lower slopes (Fig 5(i) and (ii)) at the gully mouth,



310 featuring the construction of major roads and highways (G213 and G2417), alongside the expansion of existing  
311 residential areas. Chediguan exhibits a less marked land cover transformation, owing to roads being directed  
312 through mountain tunnels. Notably, development in Xiaojia mainly surges post-earthquake up to 2010, with only  
313 minor construction activities documented thereafter (Fig 5(iii)).  
314



315 **Figure 5:** Evolution of the built environment and key infrastructure in (i) Cutou, (ii) Chediguan and (iii) Xiaojia  
316 post-earthquake between 2005 and 2019  
317

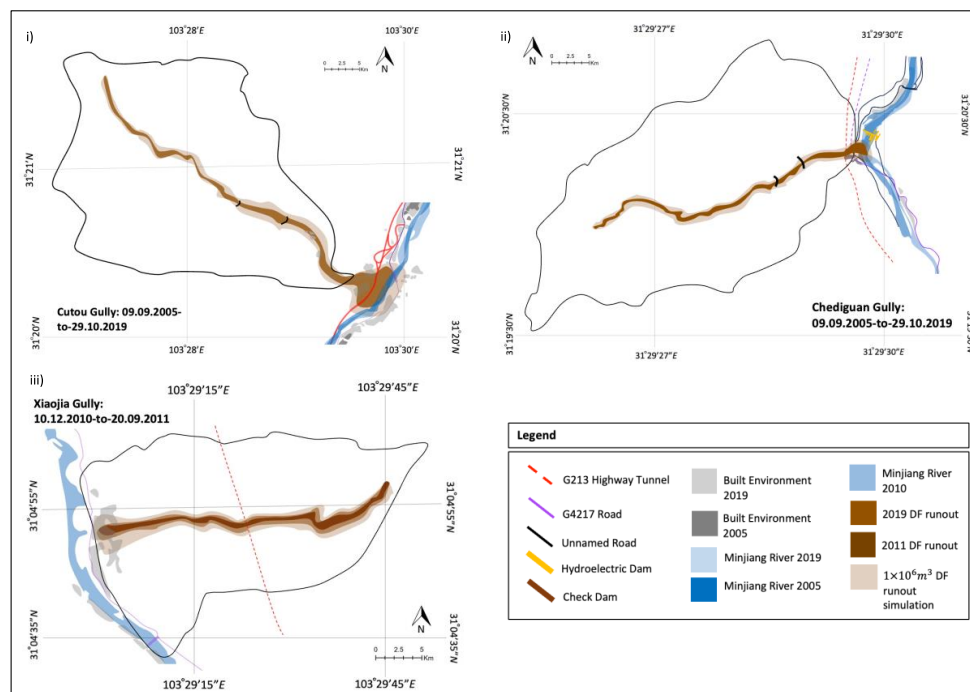
318  
319 We mapped the number of buildings impacted by debris flows that occurred within the Chediguan and Cutou  
320 gullies. At 02:00 a large-scale debris flows hit Chediguan, impacting numerous structures, at around 05:00 a  
321 similar debris flow hit Cutou with significant inundation noted. 79 of the 197 buildings (40%) in Cutou (Fig 5(i))  
322 were impacted by the flow i.e., flooded, damaged, or destroyed. Buildings in Chediguan were less impacted by  
323 that event with 7 out of the total 69 (10.1%). We combined the satellite imagery with the datasets produced by  
324 Wang (2022) which supported our observations of check dam overtopping in both Cutou and Chediguan during  
325 the 2019 event. In 2011 a similar event in Xiaojia impacted approximately 5 of the 43 (11.6%) buildings in the  
326 gully (Fig 5(iii)).  
327

### 328 4.3 Modelling exposure to post-earthquake debris flows

329  
330 Our LAHARZ simulations demonstrate a clear correlation between exposure and debris flow runoff, revealing a  
331 notable increase in building damage as runoff volumes escalate from low (10,000m<sup>3</sup>) to high (100,000m<sup>3</sup>) and  
332 extreme (1,000,000m<sup>3</sup>) scenarios across all catchments. Despite the presence of check dams, the 2019 debris flows  
333 recorded runoff volumes significantly larger than the maximum simulated volume, resulting in substantial  
334 building and infrastructural loss in Cutou (Fig 6(i)) and Chediguan (Fig 6(ii)).  
335



336

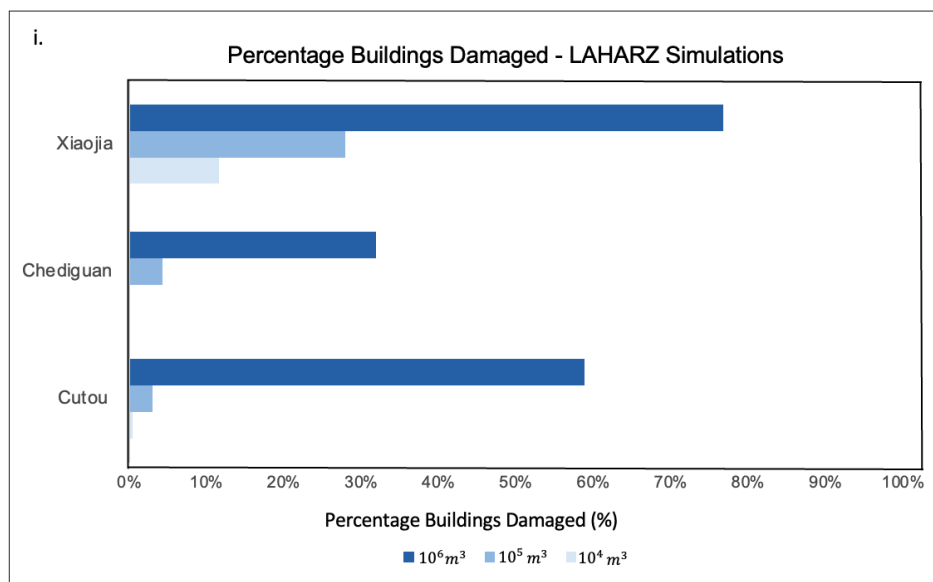


337  
338 **Figure 6:** Debris flow runouts for 2019 in Cutou (i) and Chediguan(ii) and 2011 in Xiaojia (iii) underlain by the  
339 extreme LAHARZ runout scenario. Low and high runouts are not displayed as they are not easy to visualise at  
340 map scale  
341

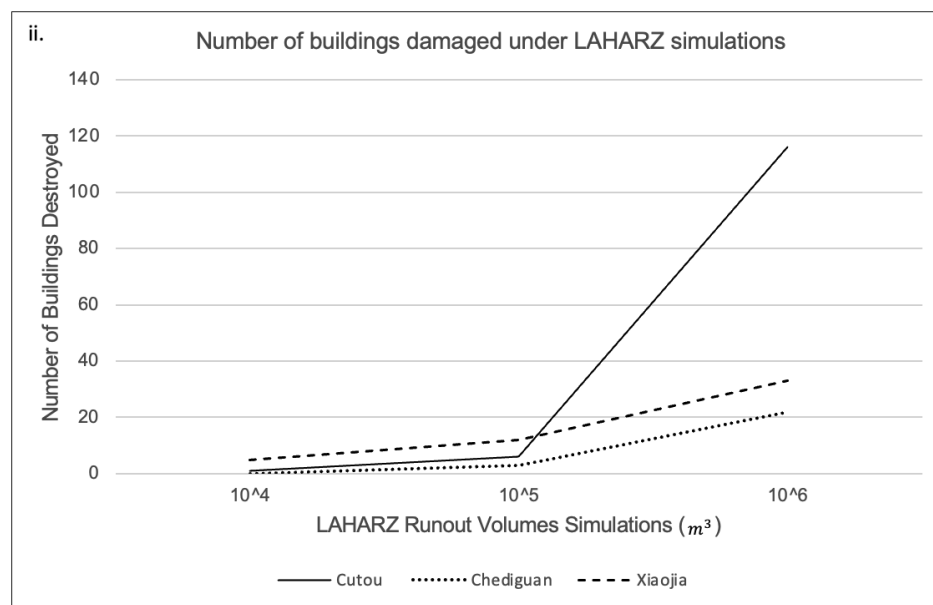
342 We examined the temporal dynamics of building changes within the three gullies in response to check dam  
343 development, while also considering the implications of the levee effect (fig 6). Our simulations revealed the  
344 effectiveness of engineered measures in mitigating exposure to debris flow events. In both Cutou and Chediguan,  
345 the presence of check dams led to reduced exposure at low and high debris flow volumes (fig 7(i) and (ii)).  
346 However, the mitigative structure provides no discernible protection against extreme debris flows. Notably, Cutou  
347 consistently exhibited elevated exposure to debris flow runout compared to Chediguan. The unengineered Xiaojia  
348 provided an informative comparison (fig 6(iii)), highlighting the effectiveness of check dams at low and high  
349 debris flow volumes. Xiaojia's post-2011 expansion appeared restrained, indicating a potential adaptive response  
350 following debris flow events. In contrast, substantial expansion occurred in Cutou and Chediguan between 2011  
351 and 2019, despite experiencing a debris flow event in 2013, suggesting the impact of check dams implemented  
352 post-2013.  
353

354 Furthermore, the incremental increase between high and extreme simulations in Xiaojia paralleled Chediguan's  
355 gradual incline, diverging from Cutou's steep escalation. Xiaojia sustained a maximum building damage of 33%  
356 under extreme scenarios, compared with 59% in Cutou and 22% in Chediguan. This discrepancy suggests that the  
357 optimal efficiency of check dams may be surpassed, urging consideration of additional factors such as the  
358 landscape's inherent resilience. Our observations underscore the nuanced variability in the effectiveness of check  
359 dams, influenced by contextual factors and landscape characteristics.  
360

361  
362  
363  
364  
365  
366  
367



368



369

370

371

372

373

374

375

376

377

378

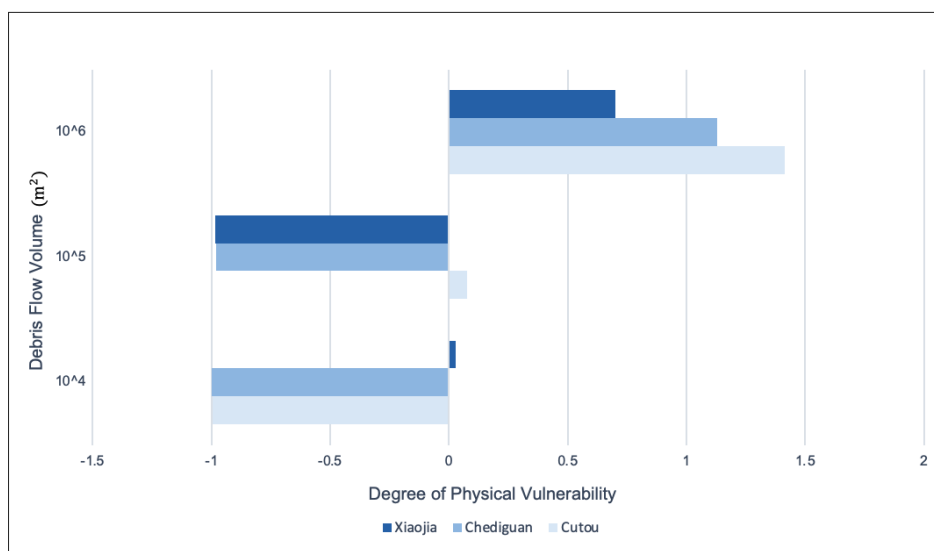
**Figure 7:** Built environment impacts from three debris flow scenarios modelled using LAHARZ at Cutou, Chediguan and Xiaoja. (i). Percentage of buildings damaged as a proportion of total buildings in each scenario. (ii) Total number of buildings damaged by each simulated debris flow

Figure 7 illustrates how a tenfold increase in runout volume corresponds to building damage, with a discernible rise in impacted building numbers noted between low and high scenarios, and a significant incline between high and extreme scenarios across all catchments. These simulations provide valuable insights into the efficacy of engineered mitigation structures. While check dams in Cutou and Chediguan effectively reduce exposure at low



379 and high runout volumes, concerns arise when surpassing the maximum capacity. Urbanization emerges as a  
380 significant contributing factor impacting exposure and future risk, with the presence of check dams during the  
381 2019 events significantly contributing to the built environment's exposure. However, to fully understand the effect  
382 of check dams and validate our statistical approach, comprehensive numerical analysis of multiple hazard events  
383 in each gully is necessary. This sub-section addresses the elements driving hazard-related risk scenarios, including  
384 the trigger event, return period, and level of damage, and underscores the importance of considering these factors  
385 when suggesting and implementing modifications.  
386

387 The exposure model is applied to historical events (2019 and 2011) and LAHARZ simulations, showcasing  
388 changes in the degree of exposure across the catchments with increasing debris flow runout volumes (Fig 8). Consistent  
389 with earlier observations in exposure, Cutou exhibits a heightened vulnerability to debris flows at 64% after the  
390 2019 event, followed by Chediguan at 52% and Xiaojia with 2% in 2011. A discernible change in building  
391 exposure is observed between the high and extreme scenarios across all catchments. The most influential factor  
392 in overall vulnerability remains the number of buildings, highlighting urbanization as a contributing factor  
393 impacting both exposure and physical vulnerability. Moreover, the presence of failed check dams in Cutou and  
394 Chediguan during the 2019 events significantly contributes to their physical vulnerability.



395 **Figure 8:** Changes in the degree of exposure with increasing runout volumes using the exposure model developed  
396 in equation 1. The 2011 and 2019 debris flows are also noted as a base marker from an observed hazard event  
397

### 398 399 **5. Discussion**

400 Post-earthquake structural interventions influence the volume and spatial distribution of sediment within the  
401 catchment. Our observations show that check dams act as local depocentres within the catchment, often storing  
402 large volumes of sediment upstream of the majority of building development. The choices made about post-  
403 earthquake development of the built environment, particularly housing, and mitigative measures like check dams,  
404 evolve rapidly without a clear approach to mitigating adverse long-term consequences of sediment retention  
405 behind dams (McGuire et al., 2017). Additionally, the processes driving geological disasters in the complex  
406 landscape of the Longmenshan occur at different timescales to the rapid socio-economic development in the region  
407 (Chen et al., 2022).  
408

409 Although our analysis focuses on smaller-scale communities, the implications drawn from our findings echo those  
410 of broader studies. For instance, Arrogante-Funes et al. (2021)'s extensive investigation into hazard mitigation  
411 strategies in larger geographical regions, drew parallels to the effectiveness and limitations of mitigation measures  
412 to debris flows. Similarly, Chen et al. (2021) provided insights into the complexities of hazard mitigation,  
413 emphasising the necessity of adaptive responses considering local contexts. This aligns with our analysis that each  
414 gully must be assessed and mitigated individually rather than collectively to account for local geological and



415 hydrological influences on mitigation effectiveness. Moreover, Li et al. (2018) examined the long-term impact of  
416 engineering interventions, noting the variability in check dams effectiveness over time. This supports our  
417 conclusion that the diminishing effectiveness of check dams is likely the result of sediment accumulation and  
418 structural degradation and highlights the necessity for their continued maintenance post-construction in addition  
419 to adaptive mitigation strategies. Furthermore, Eidsvig et al. (2014) and Tang et al. (2011) explored the interplay  
420 between socio-economic factors and hazard vulnerability, emphasising that community resilience is directly  
421 linked to economic resource availability and social cohesion. This corroborates our understanding that debris flow  
422 mitigation is a multifaceted issue, and socio-economic conditions are integral to their success. By situating our  
423 findings within the broader context delineated by these studies, we accentuate the relevance and applicability of  
424 our research beyond the confines of the specific communities under study.

425  
426 Open check dams, similar to those established in Cutou and Chediguan, play a pivotal role in bed stabilization,  
427 slope reduction, and the regulation of sediment transport (Bernard et al., 2019). However, inadequate  
428 understanding of post-earthquake debris flow characteristics has led to the failure of many newly constructed  
429 engineered structures to mitigate hazards effectively, amplifying damage instead (Chang et al., 2022). During the  
430 August 2019 debris flow, Cutou experienced the highest inundation, with 40% of surveyed structures directly  
431 affected, including critical infrastructure like the G4217 highway bridge. In Chediguan, despite a declined  
432 industrial presence, debris flow impacts affected 7% of structures. The presence of check dams in both locations  
433 contributed to raised exposure and hazard impacts during the 2019 event, with overtopping and damage to dam  
434 sections recorded.

435  
436 We conducted LAHARZ scenarios to predict potential exposure to debris flows with volumes that have been  
437 observed within the catchments and the region. Our results highlighted a clear correlation between exposure and  
438 debris flow runout, showing notable increases in building damage as runout volumes escalated from low to  
439 extreme across all catchments. We observed two key elements to the role of check dams in affecting exposure to  
440 debris flows. When empty, check dams are effective at mitigating the effects of small and medium volume debris  
441 flows. Yet, they are not effective at mitigating the largest of debris flows observed in this region. Large runout  
442 volumes in the 2019 debris flows resulted in substantial building and infrastructural loss in both Cutou and  
443 Chediguan, suggesting a negative contribution from damaged check dams. Cutou was found to be highly exposed  
444 to extreme debris flow volumes, a result of its raised development level situated at the basal slopes. The fact that  
445 Xiaojia was found to possess the least exposure to the most extreme debris flow volume suggests that there may  
446 be an adaptive component to debris flow mitigation in catchments without significant check dam development.  
447 These findings suggest that urban development and debris flow risk co-evolve based on the nature of the structural  
448 interventions the studied areas.

449  
450 Our analysis of erosion, transportation, and deposition zones for each gully revealed significant changes in  
451 landscape morphology post-earthquake, likely attributed to mobilised coseismic deposits and subsequent debris  
452 flow occurrences. The presence of check dams influenced deposition patterns, with mid-to-downstream trends  
453 indicating effective sediment retention in Cutou and Chediguan, while Xiaojia exhibited typical erosion-  
454 deposition behaviour. Our findings can be supported by a similar occurrence during the “8.13” debris flow event  
455 in Wenjiagou. The damage and subsequent failure of mitigative check dams led to the inundation of 490 houses  
456 or more recently, a debris flow in the Miansi and Weizhou townships on 27 June 2023 blocked the valley in the  
457 first instance before breaching the dam and causing 7 fatalities (Petley., 2023). Further research is thus imperative  
458 to devise appropriate mitigation approaches for post-seismic debris flows. Whilst existing literature has  
459 underscored the physical effectiveness of check dams in reducing exposure to debris flow impacts within Alpine  
460 terrains (Piton et al., 2016), it should be noted that their primary function extends beyond this to also provide  
461 socio- economic and political reassurance (Wu et al., 2012; Chen et al., 2022)

462  
463 The findings of our paper support the theory of the levee effect by demonstrating how the implementation of  
464 mitigative measures, such as check dams, can inadvertently increase exposure levels and risk perception in hazard-  
465 prone areas. The interplay between engineering solutions and the built environment as highlighted in our study  
466 through analysis of the 2011 and 2019 events as well as the LAHARZ simulations, illustrates the levee effect.  
467 Similar to previous studies on flooding and the levee effect, for example Collenteur et al (2015), our paper suggests  
468 that the perceived reduction in hazard risk due to mitigative structures can lead to increased levels of exposure  
469 due to raised development in debris flow-prone regions. This is particularly evident in the Cutou catchment. This  
470 phenomenon reflects the distorted perception of hazard risk, which ultimately drives urbanisation into vulnerable  
471 areas (Chen et al., 2015; Ao et al.,2020).

472  
473 Our LAHARZ simulations further reinforce the limitations of engineered structures as the sole mitigative measure  
474 in alpine locations; urbanisation of mountainous terrains further accentuates the balance between technological



475 advancements and geological hazards (Zhang, S et al., 2014; Zhang and Li., 2020; Luo et al., 2023). Despite the  
476 presence of check dams, our extreme runout volume resulted in significant impacts on the built environment in  
477 Cutou and Chediguan, including overtopping and dam failure. The use of these simulations emphasises the  
478 challenges of reducing exposure to at-risk structures and highlights the unpredictable nature of debris flow  
479 occurrences. Moreover, our findings relating to the altered patterns of erosion and deposition emphasise the  
480 relationship between natural topography, engineered interventions, and risk perception in post-seismic debris  
481 flows. Urbanisation exacerbates this complexity, influencing exposure and physical vulnerability through deposit  
482 remobilisation. Our LAHARZ simulations serve as a practical demonstration of the levee effect, illustrating how  
483 engineered structures may not provide adequate protection against runout volumes similar to the extreme  
484 simulation, thereby reinforcing the importance of considering the levee effect in debris flow risk management.  
485 The unpredictable nature of debris flow occurrences from pinpointing their location and timing to ascertaining  
486 their volume and velocity ultimately means that the concept of the 'levee effect' remains core to the issue of debris  
487 flows in post-seismic Sichuan (Cucchiari et al., 2019a; Tang et al., 2022).

488  
489 Whilst our findings are not able to conclusively determine the prevalence of the levee effect with regards to  
490 development in post-seismic environments like Sichuan, we are able to hypothesise this theory. From our study,  
491 we are able to posit that the implementation of mitigative check dams may inadvertently increase exposure levels  
492 to large-scale debris flow events by creating a false sense of safety. While our investigation does not fully explore  
493 this phenomenon, our outcomes highlight the limitations of solely relying on engineered interventions in reducing  
494 exposure to at-risk structures under the extreme LAHARZ scenario. Furthermore, we highlighted the complex  
495 interplay between engineering solutions and human behaviour, warranting further investigation (Papathoma-  
496 Köhle et al., 2011; Gong et al., 2021). By emphasising the challenges and limitations of engineered structures in  
497 mitigating debris flow impacts, we underscore the need for comprehensive risk management strategies that  
498 consider the complexities of urbanization and flow-based hazards in mountainous terrains.

499  
500 Despite the presence of these engineered interventions, our analysis demonstrates significant exposure levels and  
501 infrastructure damage during extreme debris flow events. This discrepancy between perceived risk reduction and  
502 actual hazard exposure underscores the need for a more comprehensive understanding of risk perception in the  
503 context of hazard mitigation strategies. Moreover, our study highlights the importance of considering human  
504 behaviour and decision-making processes in the design and implementation of risk management measures. Future  
505 research should focus on elucidating the mechanisms driving risk perception in hazard-prone areas and developing  
506 strategies to bridge the gap between perceived and actual risk to enhance the effectiveness of mitigation efforts.

507  
508

## 509 **6. Conclusion**

510 Our study investigated the impact of debris flows in Cutou, Chediguan and Xiaojia since the 2008 Wenchuan  
511 earthquake. We used high resolution satellite imagery to build a time series of building inventories between 2005  
512 and 2019. Despite recurrent debris flow occurrences between 2010 to 2013, we found increased urban  
513 development across all three gullies until 2015.

514  
515 We found significant differences between the debris flow events of 2019 and 2011. In the August 2019 debris  
516 flow, Cutou experienced the highest inundation, with 40% of surveyed structures directly affected, including  
517 critical infrastructure such as the G4217 highway bridge. In contrast, the 2011 event in Xiaojia impacted  
518 approximately 11.6% of buildings in the gully, indicating a lower level of damage compared to Cutou. The  
519 presence of check dams in Cutou and Chediguan contributed to raised exposure and hazard impacts during the  
520 2019 event, with overtopping and damage to dam sections recorded at both locations. However, despite the  
521 presence of these mitigative structures, the impact on the built environment was significant, suggesting limitations  
522 in their effectiveness, particularly during extreme runout volumes. Our Laharz simulations demonstrated a clear  
523 correlation between exposure and debris flow runout, revealing a notable increase in building damage as runout  
524 volumes increased from low to high and finally extreme scenarios across all catchments. Despite the presence of  
525 check dams, the simulations indicated that these structures were unable to reduce the impacts on the built  
526 environment, especially during extreme events. Moreover, our analysis of building damage and exposure patterns  
527 highlighted a heightened level of built environment exposure in Cutou to debris flows compared to Chediguan  
528 and Xiaojia. This susceptibility was attributed to factors such as the urbanisation, the presence of critical  
529 infrastructure, and the effectiveness of mitigative measures.

530

531 Our findings suggest that the presence and location of check dam in gully channels probably facilitated in  
532 increasing building exposure and the levee effect in addition to raising concerns about their long-term implications  
533 i.e., structural integrity, maintenance and clearing. LAHARZ modelling provides comprehension of check dam  
534 efficacy, raising concerns for Cutou and Chediguan in high-to-extreme runout events. Further, the combined use



535 of the LAHARZ GIS toolkit and exposure analysis contributes to a holistic understanding of the risk landscape,  
536 informing strategies for enhanced disaster resilience and sustainable development in vulnerable areas.  
537

538 The assumptions and subsequent considerations highlighted underpin our methodological approach in  
539 understanding how the presence of check dams, as a mitigative structure, influences land-use planning and  
540 development in hazard-prone areas. They ensure that the data outputs are comprehensive but also reflective of the  
541 inherent complexities of the study area and limitations in available data sources and analytical tools. We  
542 highlighted a relationship between the presence of engineered measures like check dams alongside the built  
543 environment, with increased debris flow impacts post-2008 earthquake in Sichuan provinces along the Minjiang..  
544 Our results emphasise the need for a multi-faceted approach integrating socio-economic development in debris  
545 flow prone regions, considering the paradoxical role of mitigative structures on public perception to hazard  
546 exposure and vulnerability. Understanding these complexities is vital for informed decision-making and effective  
547 debris flow risk management.  
548

549 Overall, our findings have indicated that the 2019 debris flow events resulted in more significant damage and  
550 higher exposure levels compared to the 2011 flow, emphasizing the need for comprehensive risk management  
551 strategies in debris flow-prone areas.  
552

#### 553 Acknowledgements

554 EH is supported by the BGS-NERC National Capability grant ‘Geosciences to tackle Global Environmental  
555 Challenges’ (NERC reference NE/X006255/1) and publishes with permission from the Executive Director of the  
556 British Geological Survey.  
557

#### 558 References

- 559 Ao, Y., Huang, K., Wang, Y., Wang, Q. and Martek, I. 2020. Influence of built environment and risk  
560 perception on seismic evacuation behavior: Evidence from rural areas affected by Wenchuan  
561 earthquake. *International journal of disaster risk reduction*: IJDRR 46(101504), p. 101504. Available at:  
562 <https://www.sciencedirect.com/science/article/pii/S2212420919313500>.  
563
- 564 Arrogante-Funes, P., Bruzón, A.G., Arrogante-Funes, F., Ramos-Bernal, R.N. and Vázquez-Jiménez, R.  
565 2021. Integration of vulnerability and hazard factors for landslide risk assessment. *International journal of*  
566 *environmental research and public health* 18(22), p. 11987. Available at:  
567 <http://dx.doi.org/10.3390/ijerph182211987>.  
568
- 569 Bernard, M., Boreggio, M., Degetto, M. and Gregoretti, C. 2019. Model-based approach for design and  
570 performance evaluation of works controlling stony debris flows with an application to a case study at Rovina di  
571 Cancia (Venetian Dolomites, Northeast Italy). *The Science of the total environment* 688, pp. 1373–1388.  
572 Available at: <https://www.sciencedirect.com/science/article/pii/S0048969719325288>.  
573
- 574 Brown, C. F. *et al.* Dynamic world, near real-time global 10 m land use land cover mapping. *Scientific Data* 9,  
575 251 (2022)  
576
- 577 Chang, M., Luo, C., Wu, B. and Xiang, L. 2022. Catastrophe process of outburst debris flow triggered by the  
578 landslide dam failure. *Journal of hydrology* 609(127729), p. 127729. Available at:  
579 <https://www.sciencedirect.com/science/article/pii/S0022169422003043>.  
580
- 581 Chen, N.-S., Hu, G.-S., Deng, M.-F., Zhou, W., Yang, C.-L., Han, D. and Deng, J.-H. 2011. Impact of  
582 earthquake on debris flows — a case study on the Wenchuan earthquake. *Journal of earthquake and*  
583 *tsunami* 05(05), pp. 493–508. Available at: <http://dx.doi.org/10.1142/s1793431111001212>.  
584
- 585 Chen, X., Cui, P., You, Y., Chen, J. and Li, D. 2015. Engineering measures for debris flow hazard mitigation  
586 in the Wenchuan earthquake area. *Engineering geology* 194, pp. 73–85. Available at:  
587 <https://www.sciencedirect.com/science/article/pii/S0013795214002579>.  
588
- 589 Chen, M. *et al.* 2021. Quantitative assessment of physical fragility of buildings to the debris flow on 20 August  
590 2019 in the Cutou gully, Wenchuan, southwestern China. *Engineering geology* 293(106319), p. 106319.  
591 Available at: <https://www.sciencedirect.com/science/article/pii/S0013795221003306>  
592



- 593 Chen, Y., Song, J., Zhong, S., Liu, Z. and Gao, W. 2022. Effect of destructive earthquake on the population-  
594 economy-space urbanization at county level-a case study on Dujiangyan county, China. Sustainable cities and  
595 society 76(103345), p. 103345. Available at: <http://dx.doi.org/10.1016/j.scs.2021.103345>.  
596
- 597 Collenteur, R. A., de Moel, H., Jongman, B., & Di Baldassarre, G. (2015). The failed-levee effect: Do societies  
598 learn from flood disasters? *Natural Hazards (Dordrecht, Netherlands)*, 76(1), 373–388.  
599 <https://doi.org/10.1007/s11069-014-1496-6>  
600
- 601 Costa, J.E. 1984. Physical geomorphology of debris flows. In: *Developments and Applications of*  
602 *Geomorphology*. Berlin, Heidelberg: Springer Berlin Heidelberg, pp. 268–269. Available at:  
603 [http://dx.doi.org/10.1007/978-3-642-69759-3\\_9](http://dx.doi.org/10.1007/978-3-642-69759-3_9).  
604
- 605 Couvert, B., Lefebvre, B., Lefort, P., & Morin, E. (1991). Etude générale sur les seuils de correction  
606 torrentielle et les plages de dépôts. *Houille Blanche*, 77(6), 449–456. <https://doi.org/10.1051/lhb/1991043>  
607
- 608 Cruden, D.M. and Varnes, D.J. 1996. Landslides: Investigation and Mitigation. Chapter 3—Landslide Types  
609 and Processes. Transportation research board special report, 247. In: *Transportation research board special*  
610 *report (247)*.  
611
- 612 Cucchiario, S. et al. 2019a. Geomorphic effectiveness of check dams in a debris-flow catchment using multi-  
613 temporal topographic surveys. *Catena* 174, pp. 73–83. Available at:  
614 <https://www.sciencedirect.com/science/article/pii/S0341816218304910>.  
615
- 616 Cucchiario, S., Cazorzi, F., Marchi, L., Crema, S., Beinart, A. and Cavalli, M. 2019b. Multi-temporal analysis of  
617 the role of check dams in a debris-flow channel: Linking structural and functional  
618 connectivity. *Geomorphology (Amsterdam, Netherlands)* 345(106844), p. 106844. Available at:  
619 <https://www.sciencedirect.com/science/article/pii/S0169555X1930323X>.  
620
- 621 Cui, P., Wei, F. Q., He, S. M., You, Y., Chen, X. Q., Li, Z. L., et al. (2008). Mountain Disasters Induced by the  
622 Earthquake of May 12 in Wenchuan and the Disasters Mitigation. *J. Mountain Sci.* 26 (3), 280–282.  
623 doi:10.35123/geo-expo\_2017\_4  
624
- 625 Dai, Z., Huang, Y., Cheng, H. and Xu, Q. 2017. SPH model for fluid–structure interaction and its application to  
626 debris flow impact estimation. *Landslides* 14(3), pp. 917–928. Available at: [http://dx.doi.org/10.1007/s10346-](http://dx.doi.org/10.1007/s10346-016-0777-4)  
627 [016-0777-4](http://dx.doi.org/10.1007/s10346-016-0777-4).  
628
- 629 Eidsvig, U.M.K., Papatoma-Köhle, M., Du, J., Glade, T. and Vangelsten, B.V. 2014. Quantification of model  
630 uncertainty in debris flow vulnerability assessment. *Engineering geology* 181, pp. 15–26. Available at:  
631 <https://www.sciencedirect.com/science/article/pii/S0013795214002051>.  
632
- 633 Fan, X. et al. 2018. What we have learned from the 2008 Wenchuan Earthquake and its aftermath. A decade of  
634 research and challenges. *Engineering geology* 241, pp. 25–32. Available at:  
635 <https://www.sciencedirect.com/science/article/pii/S0013795218307233>.  
636
- 637 Fan, X., Scaringi, G., Domènech, G., Yang, F., Guo, X., Dai, L., He, C., Xu, Q., and Huang, R. 2019a. Two  
638 multi-temporal datasets that track the enhanced landsliding after the 2008 Wenchuan earthquake, *Earth Syst.*  
639 *Sci. Data*, 11, 35–55, <https://doi.org/10.5194/essd-11-35-2019>  
640
- 641 Fan, X., Scaringi, G., Korup, O., West, A. J., van Westen, C. J., Tanyas, H., Niels Hovius, Tristram C. Hales,  
642 Randall W. Jibson, Kate E. Allstadt, Limin Zhang, Stephen G. Evans, Chong Xu10, Gen Li4, Xiangjun Pei,  
643 Qiang Xu1, and Runqiu Huang. 2019b. Earthquake-induced chains of geologic hazards: Patterns, mechanisms,  
644 and impacts. *Reviews of Geophysics*, 57, 421–503. <https://doi.org/10.1029/2018RG000626>  
645
- 646 Farr, T. G., et al. (2007), The Shuttle Radar Topography Mission, *Rev. Geophys.*, 45, RG2004,  
647 doi:10.1029/2005RG000183.  
648
- 649 Fell, R., Corominas, J., Bonnard, C., Cascini, L., Leroi, E., & Savage, W. Z. 2008. Guidelines for landslide  
650 susceptibility, hazard, and risk zoning for land use planning. *Engineering Geology*, 102(3–4), 85–98.  
651 <https://doi.org/10.1016/j.enggeo.2008.03.022>



- 652 Francis, O. Fan, X., Hales, T., Hopley, D., Xu, Q., Huang, R. (2022) ‘The fate of sediment after a large  
653 earthquake’, *Journal of Geophysical Research: Earth Surface*, 127(3). doi:10.1029/2021jf006352
- 654 Gong, X.-L., Chen, X.-Q., Chen, K.-T., Zhao, W.-Y. and Chen, J.-G. 2021. Engineering planning method and  
655 control modes for debris flow disasters in scenic areas. *Frontiers in earth science* 9. Available at:  
656 <http://dx.doi.org/10.3389/feart.2021.712403>
- 657 Google Earth Pro. Version 9.189.0.0 “Location of Cutou gully, Chediguan Gully and Xiaojia Gully,  
658 Sichuan, China”. Image taken 2020. Accessed June 2, 2023.
- 659 Guo, X., Cui, P., Li, Y., Ma, L., Ge, Y., and Mahoney, W.B. 2016. Intensity–duration threshold of rainfall-  
660 triggered debris flows in the Wenchuan Earthquake affected area, China. *Geomorphology* (Amsterdam,  
661 Netherlands) 253, pp. 208–216. Available at: <http://dx.doi.org/10.1016/j.geomorph.2015.10.009>.
- 662 Guzzetti, F. et al. 2008. The rainfall intensity-duration control of shallow landslides and debris flows: An  
663 update. *Landslides* 5(1), pp. 3–17. [Doi: 10.1007/s10346-007-0112-1](https://doi.org/10.1007/s10346-007-0112-1).
- 664 Hao, P. Hooimeijer, P. Sliuzas, R and Geertma, S. 2013 ‘What drives the spatial development of urban villages  
665 in China?’, *Urban Studies*, 50(16), pp. 3394–3411. doi:10.1177/0042098013484534
- 666 Hao, P. (2012) *Spatial evolution of urban villages in Shenzhen*. dissertation. University of Utrecht. Available at:  
667 [https://webapps.itc.utwente.nl/librarywww/papers\\_2012/phd/puhao.pdf](https://webapps.itc.utwente.nl/librarywww/papers_2012/phd/puhao.pdf)
- 668
- 669 He, N., Fu, Q., Zhong, W., Yang, Z., Cai, X. and Xu, L. 2022. Analysis of the formation mechanism of debris  
670 flows after earthquakes – A case study of the Legugou debris flow. *Frontiers in ecology and evolution* 10.  
671 Available at: <http://dx.doi.org/10.3389/fevo.2022.1053687>
- 672 Horton, A.J. et al. (2019) ‘Identifying post-earthquake debris flow hazard using Massflowx’, *Engineering  
673 Geology*, 258, p. 105134. doi:10.1016/j.enggeo.2019.05.011
- 674 Hu, K.H., Cui, P., and Zhang, J.Q. 2012. Characteristics of damage to buildings by debris flows on 7 August  
675 2010 in Zhouqu, Western China. *Natural hazards and earth system sciences* 12(7), pp. 2209–2217. Available  
676 at: <https://nhess.copernicus.org/articles/12/2209/2012/nhess-12-2209-2012.pdf>.
- 677
- 678 Huang, R. Q., & Li, W. L. 2009. Analysis of the geo-hazards triggered by the 12 May 2008 Wenchuan  
679 Earthquake, China. *Bulletin of Engineering Geology and the Environment*, 68(3), 363–371.  
680 <https://doi.org/10.1007/s10064-009-0207-0>
- 681
- 682 Huang, R., Pei, X., Fan, X., Zhang, W., Li, S. and Li, B. 2012. The characteristics and failure mechanism of  
683 the largest landslide triggered by the Wenchuan earthquake, May 12, 2008, China. *Landslides* 9(1), pp. 131–  
684 142. Available at: <http://dx.doi.org/10.1007/s10346-011-0276-6>.
- 685
- 686 Huang, R. and Li, W. 2014. Post-earthquake landsliding and long-term impacts in the Wenchuan earthquake  
687 area, China. *Engineering geology* 182, pp. 111–120. Available at:  
688 <http://dx.doi.org/10.1016/j.enggeo.2014.07.008>.
- 689
- 690 Hübl, J. and Fiebiger, G. 2005. Chap. 18 - Debris-flow mitigation measures. In: *Debris-flow Hazards and  
691 Related Phenomena*. Berlin, Heidelberg: Springer Berlin Heidelberg, pp. 445–487. Available at:  
692 [https://link.springer.com/content/pdf/10.1007/3-540-27129-5\\_18.pdf](https://link.springer.com/content/pdf/10.1007/3-540-27129-5_18.pdf)
- 693
- 694 Ivanov, P., Geological Institute, Bulgarian Academy of Sciences, Acad. Georgi Bonchev Str., Bl. 24, 1113  
695 Sofia, Bulgaria, Dobrev, N., Berov, B., Frantzova, A., Krastanov, M., Nankin, R., Geological Institute,  
696 Bulgarian Academy of Sciences, Acad. Georgi Bonchev Str., Bl. 24, 1113 Sofia, Bulgaria, & Geological  
697 Institute, Bulgarian Academy of Sciences, Acad. Georgi Bonchev Str., Bl. 24, 1113 Sofia, Bulgaria. (2022).  
698 Landslide risk for the territory of Bulgaria by administrative districts. *Geologica Balkanica*, 51(3), 21–28.  
699 <https://doi.org/10.52321/geolbalc.51.3.21>
- 700



- 701 Iverson, R.M., Schilling, S.R. and Vallance, J.W., 1998, Objective delineation of areas at risk from inundation  
702 by lahars: Geological Society of America Bulletin, V 110, no.8, p. 972-984.
- 703 Jiang, W., Deng, Y., Tang, Z., Cao, R., Chen, Z. and Jia, K. 2016. Adaptive capacity of mountainous rural  
704 communities under restructuring to geological disasters: The case of Yunnan Province. Journal of rural  
705 studies 47, pp. 622–629. Available at: <http://dx.doi.org/10.1016/j.jrurstud.2016.05.002>.
- 706 Kean, J.W. et al. 2019. Inundation, flow dynamics, and damage in the 9 January 2018 Montecito debris-flow  
707 event, California, USA: Opportunities and challenges for post-wildfire risk assessment. *Geosphere* 15(4), pp.  
708 1140–1163. Available at: <http://dx.doi.org/10.1130/ges02048.1>.
- 709 Li, C., Wang, M. and Liu, K. 2018. A decadal evolution of landslides and debris flows after the Wenchuan  
710 earthquake. *Geomorphology (Amsterdam, Netherlands)* 323, pp. 1–12. Available at:  
711 <http://dx.doi.org/10.1016/j.geomorph.2018.09.010>.
- 712 Li, N., Tang, C., Zhang, X., Chang, M., Shu, Z. and Bu, X. 2021b. Characteristics of the disastrous debris flow  
713 of Chediguan gully in Yinxing town, Sichuan Province, on August 20, 2019. *Scientific reports* 11(1). Available  
714 at: <https://www.nature.com/articles/s41598-021-03125-x>
- 715 Liu, J., You, Y., Chen, X., Liu, J. and Chen, X. 2014. Characteristics and hazard prediction of large-scale  
716 debris flow of Xiaojia Gully in Yingxiu Town, Sichuan Province, China. *Engineering geology* 180, pp. 55–67.  
717 Available at: <https://www.sciencedirect.com/science/article/pii/S0013795214000702>
- 718 Liu, J., You, Y., Chen, X. and Chen, X. 2016. Mitigation planning based on the prediction of river blocking by  
719 a typical large-scale debris flow in the Wenchuan earthquake area. *Landslides* 13(5), pp. 1231–1242. Available  
720 at: <http://dx.doi.org/10.1007/s10346-015-0615-0>
- 721 Liu, J., Mason, P.J. and Bryant, E.C. 2018. Regional assessment of geohazard recovery eight years after the  
722 Mw7.9 Wenchuan earthquake: a remote-sensing investigation of the Beichuan region. *International journal of*  
723 *remote sensing* 39(6), pp. 1671–1695. Available at: <http://dx.doi.org/10.1080/01431161.2017.1410299>.
- 724 Luo, H.Y., Fan, R.L., Wang, H.J., and Zhang, L.M. 2020. Physics of building vulnerability to debris flows,  
725 floods, and earth flows. *Engineering geology* 271(105611), p. 105611. Available at:  
726 <https://www.sciencedirect.com/science/article/pii/S0013795219322227>.
- 727 Luo, H.Y., Zhang, L.M., Zhang, L.L., He, J., and Yin, K.S. 2023. Vulnerability of buildings to landslides: The  
728 state of the art and future needs. *Earth-science reviews* 238(104329), p. 104329. Available at:  
729 <https://www.sciencedirect.com/science/article/pii/S0012825223000181>.
- 730 Mattia Marconcini, Annetkatrin Metz-Marconcini, Thomas Esch and Noel Gorelick. Understanding Current  
731 Trends in Global Urbanisation - The World Settlement Footprint Suite. *GI\_Forum* 2021, Issue 1, 33-38  
732 (2021) <https://austriaca.at/0xc1aa5576%20x003c9b4c.pdf>
- 733 McGuire, L.A., Rengers, F.K., Kean, J.W. and Staley, D.M. 2017. Debris flow initiation by runoff in a recently  
734 burned basin: Is grain-by-grain sediment bulking or en masse failure to blame?: DEBRIS FLOW  
735 INITIATION. *Geophysical research letters* 44(14), pp. 7310–7319. Available at:  
736 <http://dx.doi.org/10.1002/2017gl074243>.
- 737 OpenStreetMap contributors. OpenStreetMap database [PostgreSQL via API]. OpenStreetMap Foundation:  
738 Cambridge, UK. 2024 [cited 20 Jul 2023]. © OpenStreetMap contributors. Available under the Open Database  
739 Licence from: [openstreetmap.org](https://www.openstreetmap.org). Data mining by Overpass turbo. Available at <https://www.openstreetmap.org>
- 740 Papathoma-Köhle, M., Kappes, M., Keiler, M. and Glade, T. 2011. Physical vulnerability assessment for alpine  
741 hazards: state of the art and future needs. *Natural hazards (Dordrecht, Netherlands)* 58(2), pp. 645–680.  
742 Available at: <http://dx.doi.org/10.1007/s11069-010-9632-4>.



- 743 Peng, M., Zhang, L.M., Chang, D.S. and Shi, Z.M. 2014. Engineering risk mitigation measures for the landslide  
744 dams induced by the 2008 Wenchuan earthquake. *Engineering geology* 180, pp. 68–84. Available at:  
745 <https://www.sciencedirect.com/science/article/pii/S0013795214000696>.  
746
- 747 Petley, D. 2023. *The 27 June 2023 landslide at Miansi, Sichuan Province, China*. Available at:  
748 <https://blogs.agu.org/landslideblog/2023/06/29/miansi-landslide-1/>  
749
- 750 Shen, P., Zhang, L. M., Chen, H. X., & Gao, L. (2017). Role of vegetation restoration in mitigating hillslope  
751 erosion and debris flows. *Engineering Geology*, 216, 122–133. <https://doi.org/10.1016/j.enggeo.2016.11.019>
- 752 Shu, B., Chen, Y., Amani-Beni, M. and Zhang, R. 2022. Spatial distribution and influencing factors of  
753 mountainous geological disasters in southwest China: A fine-scale multi-type assessment. *Frontiers in*  
754 *environmental science* 10. Available at: <http://dx.doi.org/10.3389/fenvs.2022.1049333>.
- 755 Tang, C., Rengers, N., van Asch, T.W.J., Yang, Y.H. and Wang, G.F. 2011. Triggering conditions and  
756 depositional characteristics of a disastrous debris flow event in Zhouqu city, Gansu Province, northwestern  
757 China. *Natural hazards and earth system sciences* 11(11), pp. 2903–2912. Available at:  
758 <https://nhess.copernicus.org/articles/11/2903/2011/nhess-11-2903-2011.pdf>.  
759
- 760 Tang, C., Van Westen, C.J., Tanyas, H. and Jetten, V.G. 2016. Analysing post-earthquake landslide activity  
761 using multi-temporal landslide inventories near the epicentral area of the 2008 Wenchuan earthquake. *Natural*  
762 *hazards and earth system sciences* 16(12), pp. 2641–2655. Available at: [http://dx.doi.org/10.5194/nhess-16-](http://dx.doi.org/10.5194/nhess-16-2641-2016)  
763 [2641-2016](http://dx.doi.org/10.5194/nhess-16-2641-2016).  
764
- 765 Tang, Y. et al. 2022. Assessing debris flow risk at a catchment scale for an economic decision based on the  
766 LiDAR DEM and numerical simulation. *Frontiers in earth science* 10. Available at:  
767 <http://dx.doi.org/10.3389/feart.2022.821735>  
768
- 769 Thouret, J.-C., Antoine, S., Magill, C. and Ollier, C. 2020. Lahars and debris flows: Characteristics and  
770 impacts. *Earth-science reviews* 201(103003), p. 103003. Available at:  
771 <http://dx.doi.org/10.1016/j.earscirev.2019.103003>.  
772
- 773 Wang, C., Li, S. and Esaki, T. 2008. GIS-based two-dimensional numerical simulation of rainfall-induced  
774 debris flow. Available at: <https://nhess.copernicus.org/articles/8/47/2008/nhess-8-47-2008.pdf>
- 775 Wei, L., Hu, K. and Liu, J. 2022. Automatic identification of buildings vulnerable to debris flows in Sichuan  
776 Province, China, by GIS analysis and Deep Encoding Network methods. *Journal of flood risk*  
777 *management* 15(4). Available at: <http://dx.doi.org/10.1111/jfr3.12830>
- 778 Wei, L., Hu, K. and Liu, J. 2021 ‘Quantitative analysis of the debris flow societal risk to people inside buildings  
779 at different times: A case study of Luomo Village, Sichuan, Southwest China’, *Frontiers in Earth Science*, 8.  
780 doi:10.3389/feart.2020.627070.
- 781 Wei, L., Hu, K.-H. and Hu, X.-D. 2018. Rainfall occurrence and its relation to flood damage in China from  
782 2000 to 2015. *Journal of mountain science* 15(11), pp. 2492–2504. Available at:  
783 <http://dx.doi.org/10.1007/s11629-018-4931-4>
- 784 World Settlement Footprint Evolution data (1985-2015) ©DLR [cited Jul 2023]. 2019 All rights  
785 reserved. <https://geoservice.dlr.de/web/maps/eoc/wsfevolution>  
786
- 787 Yan, Y., Ge, Y.G., Zhang, J.Q. and Zeng, C. 2014. Research on the debris flow hazards in Cutou Gully,  
788 Wenchuan County on July 10, 2013. *Journal of Catastrophology*, 29(3), pp.229-234.
- 789 Zeng, Q.L., Yue, Z.Q., Yang, Z.F. and Zhang, X.J. 2009. A case study of long-term field performance of  
790 check-dams in mitigation of soil erosion in Jiangjia stream, China. *Environmental geology* 58(4), pp. 897–911.  
791 Available at: <http://dx.doi.org/10.1007/s00254-008-1570-z>.



792 Zeng, C., Cui, P., Su, Z., Lei, Y. and Chen, R. 2015. Failure modes of reinforced concrete columns of buildings  
793 under debris flow impact. *Landslides* 12(3), pp. 561–571. Available at: [http://dx.doi.org/10.1007/s10346-014-](http://dx.doi.org/10.1007/s10346-014-0490-0)  
794 [0490-0](http://dx.doi.org/10.1007/s10346-014-0490-0)

795 Zhang, S. 2014. Assessment of human risks posed by cascading landslides in the Wenchuan earthquake area.  
796 (Hong Kong): Hong Kong University of Science and Technology.

797 Zhang, Z. and Li, Y. 2020. Coupling coordination and spatiotemporal dynamic evolution between urbanization  
798 and geological hazards—A case study from China. *The Science of the total environment* 728(138825), p.  
799 138825. Available at: <http://dx.doi.org/10.1016/j.scitotenv.2020.138825>.

800 Zhu, Cheng, Bao, Chen, and Huang 2022. Shaking table tests on the seismic response of slopes to near-fault  
801 ground motion. *Geomechanics and engineering* 29(2), pp. 133–143. Available at:  
802 <http://dx.doi.org/10.12989/gae.2022.29.2.133>.

803 Zou, Q., Cui, P., He, J., Lei, Y. and Li, S. 2019. Regional risk assessment of debris flows in China—An HRU-  
804 based approach. *Geomorphology (Amsterdam, Netherlands)* 340, pp. 84–102. Available at:  
805 <https://www.sciencedirect.com/science/article/pii/S0169555X19301849>

806  
807

## 808 **Statements & Declarations**

809

### 810 **Conflict of Interest**

811 The authors disclose no financial or non-financial interests of competing interest during the preparation of this  
812 manuscript.

813

### 814 **Author Contribution**

815 All authors contributed to the study conception and design. Material preparation, data collection and analysis were  
816 performed by Isabelle Utley, Tristram Hales and Ekbal Hussain. The first draft of the manuscript was written by  
817 Isabelle Utley and all authors commented on previous versions of the manuscript. All authors read and approved  
818 the final manuscript